Effect of inversion asymmetry on the conduction subbands in GaAs-$Ga_{1-x}Al_xAs$ heterostructures

P. Pfeffer
Institute of Physics, Polish Academy of Sciences, Aleja Lotnikow 32/46, 02-668 Warsaw, Poland
(Received 15 October 1998)

Spin splitting of conduction subbands in GaAs-$Ga_{1-x}Al_xAs$ heterostructures due to both bulk and structure inversion asymmetry is considered theoretically using a five-level $\mathbf{k}\cdot\mathbf{p}$ model. A formula for the splitting related to the structure inversion asymmetry is derived and it is explicitly demonstrated that this splitting is not proportional to the average electric field in the system. The theory is shown to describe well existing Raman data on anisotropic spin splitting in GaAs-$Ga_{1-x}Al_xAs$ heterostructures for various directions of the Fermi wave vector. It is shown that the splitting is dominated by the bulk inversion asymmetry at low two-dimensional electron densities and by the structure inversion asymmetry at high densities. Various simplifications of the presented complete theory are discussed. [S0163-1829(99)01523-4]

I. INTRODUCTION

Spin splitting of electric subbands in III-V semiconducting heterostructures has attracted in recent years considerable and continuously growing theoretical and experimental interest. In a crystal with bulk inversion asymmetry (BIA) the energy bands are spin split for a given direction of the wave vector $\mathbf{k}$ (see Ref. 1, and references therein). In heterostructures the spin splitting may also occur as a result of the structure inversion asymmetry (SIA), as first pointed out by Bychkov and Rashba.[2] The history of the subject is quite controversial. In the first theory for metal-oxide–semiconductor structure Ohkawa and Uemura[3] concluded that in a system with an asymmetric potential $V(z)$ the spin splitting is proportional to $-\partial V/\partial z = qE$. However, as remarked by Darr, Kotthaus, and Ando,[4] in bound states the average value of electric field vanishes. Lassnig[5] considered the effect of SIA in GaAs-$Ga_{1-x}Al_xAs$ heterostructure within an incomplete five-level $\mathbf{k}\cdot\mathbf{p}$ model, taking into account a mass discontinuity at the interface and assuming that the average electric field in the structure vanishes. Malcher, Lommer, and Rossler[6] took into account both BIA and SIA and pointed out that the mass discontinuity in a heterostructure results in an additional force. Since it is the mean value of the total force that vanishes in a bound state, the average electric field is small but nonzero. The authors of Ref. 6 underestimated the SIA mechanism and concluded that in GaAs-$Ga_{1-x}Al_xAs$ heterostructures BIA provides the dominant source of the spin splitting. Sobkowicz[7] treated SIA in narrow-gap heterostructures and showed that boundary conditions involve spin terms (see also Bastard, Brum, and Ferreira[8]). Eppenga and Schurmann[9] calculated an anisotropy of the subband splitting (for various directions of $\mathbf{k}$) due to BIA in GaAs/AlAs symmetric quantum wells. Winkler and Roessler[10] recognized that the theory must take into account the band offsets, which results in almost zero value of an average electric field. Andrada e Silva, La Rocca, and Bassani[11] followed the initial approach of Ohkawa and Uemura.[3] Pfeffer and Zawadzki[12,13] described the spin splitting in GaAs-$Ga_{1-x}Al_xAs$ heterostructures within the complete five level $\mathbf{k}\cdot\mathbf{p}$ theory, which allows one to treat both SIA and BIA mechanisms, and showed that both of them are important in the above system. Unfortunately, deduced experimental splittings quoted in Refs 12,13, were twice higher than the real values (see below).

On the experimental side there exists an attempt to measure the spin splitting in GaAs-$Ga_{1-x}Al_xAs$ at $B=0$ by means of spin resonance (Stein, von Klitzing, and Weimann[14]), an observation of the spin precession using antilocalization in the same system by Dresselhaus *et al.*,[15] and Knap *et al.*,[16] and a direct measurement of the spin splitting with the use of Raman scattering by Jusserand *et al.*[17] and Richards *et al.*[18] There exist measurements on other systems, for which the spin splitting was determined by beatings of the Shubnikov–de Haas oscillations at low magnetic fields.[19,20] More recently it has become possible to influence the spin splittings in heterostructures by applying external electric fields.[21–23]

In spite of the explicit statements that in a bound state the average electric field is exactly or nearly zero (see Refs. 4,5,12,13,24,25), it is still often claimed that the spin splitting due to SIA (Bychkov-Rashba) mechanism is proportional to the average field (see Refs. 11,16,20–22). This is frequently accompanied by an erroneous omission of the potential discontinuities at the interfaces.

The purpose of the present work is threefold. First, we go beyond the perturbation theory, developed in Refs. 12,13, in order to describe more precisely the spin splitting in III-V heterostructures within the five-level $\mathbf{k}\cdot\mathbf{p}$ model. Second, an analytical formula for the spin splitting due to SIA mechanism is derived, which shows explicitly that the average electric field contributes only a very small portion of the total splitting due to inversion asymmetry. Third, we describe the experimental data of Refs. 17,18 on anisotropic conduction band spin splittings in GaAs-$Ga_{1-x}Al_xAs$ heterostructures, deducing correctly the relation between the Raman splittings and the energy spin splittings.

II. THEORY

Our approach is based on the $\mathbf{k}\cdot\mathbf{p}$ theory for the electron in a periodic potential V_0 in the presence of spin-orbit inter-

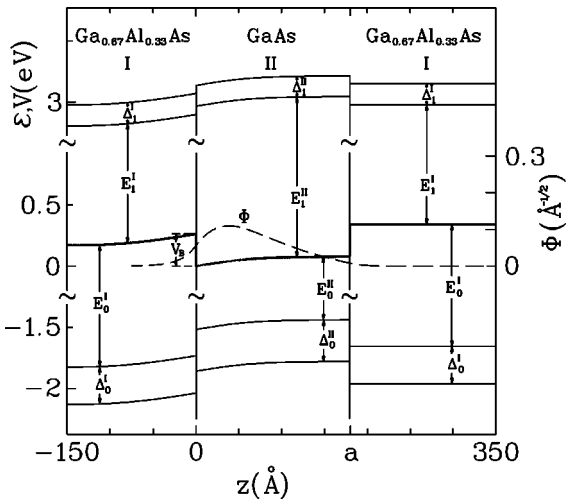

FIG. 1. Potential profiles of the conduction and the valence bands in the modulation-doped $Ga_{0.67}Al_{0.33}As/GaAs/Ga_{0.67}Al_{0.33}As$ quantum well (left scale), and the wave function of the ground conduction subband (right scale) *versus* distance along the growth direction z.

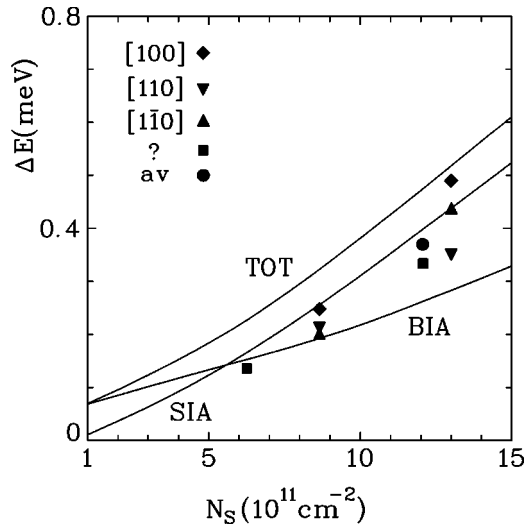

FIG. 2. Spin splitting of the lowest subband in $GaAs/Ga_{0.67}Al_{0.33}As$ heterostructure averaged over $\mathbf{k}_F$ directions versus electron density. The solid lines are theoretical: BIA, calculated for bulk inversion asymmetry alone; SIA, structure inversion asymmetry alone; TOT, both mechanisms ($N_{\mathrm{depl}}=0$). The full points are from the Raman experiments (after Refs. 17,18) for various $\mathbf{k}_F$ directions.

action. We consider a five level model (5LM) of Γ_8^c, Γ_7^c, Γ_6^c, Γ_8^v, Γ_7^v levels at $k=0$. The initial band-edge Luttinger-Kohn periodic functions u_l are chosen according to Ref. 1. These functions diagonalize the spin orbit within (Γ_8^c, Γ_7^c) and (Γ_8^v, Γ_7^v) multiplets. As a consequence, due to inversion asymmetry of the zinc blende lattice, there exists also a spin-orbit coupling $\overline{\Delta}$ between the above multiplets (Pollak *et al.*[26]). The remaining bands are neglected. The $\mathbf{k}\cdot\mathbf{p}$ theory for the bulk is then modified by the presence of a heterostructure potential $V(z)$. If this potential is slowly varying within the unit cell, it appears only on the diagonal of the $\mathbf{k}\cdot\mathbf{p}$ matrix. The initial 14×14 Hamiltonian has the form of Eq. (6) of Ref. 1, in which k_z is replaced by $-i\partial/\partial z$, all diagonal terms contain in addition $V(z)$, and the expansion coefficients c_l are replaced by the envelope functions $f_l(\mathbf{r})=\exp(ik_x x+ik_y y)\Phi_l(z)$.

We further transform the initial matrix, requiring the non-vanishing off-diagonal matrix elements to be linear in $\hat{k}_i$, which facilitates substitutional or perturbative solutions. This requires the following transformation of the initial basis:

$$
\begin{aligned}
U_{1(8)}&=c_1u_{1(8)}+\Delta' Au_{5(12)},\\
U_{2(9)}&=c_1u_{2(9)}+\Delta' Au_{6(13)},\\
U_{3(10)}&=c_2u_{3(10)}-2\Delta' Bu_{7(14)},\\
U_{4(11)}&=u_{4(11)},\\
U_{5(12)}&=c_1u_{5(12)}-\Delta' Au_{1(8)},\\
U_{6(13)}&=c_1u_{6(13)}-\Delta' Au_{2(9)},\\
U_{7(14)}&=c_2u_{7(14)}+2\Delta' Bu_{3(10)},
\end{aligned}
\tag{1}
$$

where $A=1/(G_1-E_0)$, $B=1/(E_1-G_0)$, $\Delta'=\overline{\Delta}/3$, and c_1,c_2 are the normalization coefficients. Here $G_1=E_1+\Delta_1$ and $G_0=E_0+\Delta_0$, in which E_i are the energy gaps and Δ_i the spin-orbit energies (see Fig. 1). The interband spin-orbit energy $\overline{\Delta}$ is defined in Ref. 1. Here and in the following we neglect small corrections introduced by $\overline{\Delta}$ into the band-edge energies [see Eq. (8) of Ref. 1].

The resulting eigenvalue differential matrix in the basis (1) is given by Eq. (2):

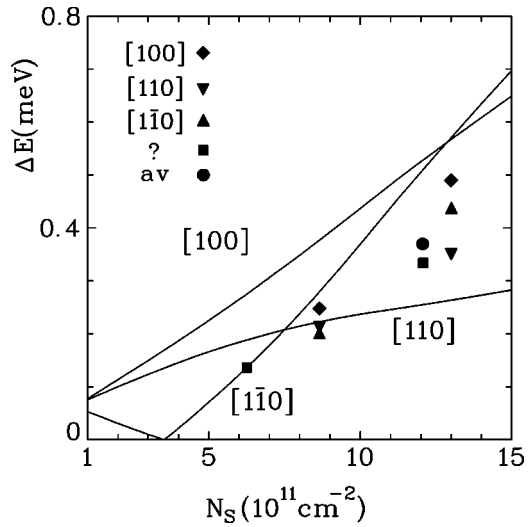

FIG. 3. Spin splitting of the lowest subband in $GaAs/Ga_{0.67}Al_{0.33}As$ heterostructure versus electron density. Theoretical curves are calculated for $\mathbf{k}_F\|[110]$, $\mathbf{k}_F\|[1\bar{1}0]$, and $\mathbf{k}_F\|[100]$, taking $N_{\mathrm{depl}}=0$. Experimental values are after Refs. 17 and 18 for the indicated directions of $\mathbf{k}_F$.

$$
\begin{bmatrix}
G_1-\lambda & 0 & 0 & -\sqrt{\frac{2}{3}}p_2\hat{k}_z & 0 & Q\hat{k}_z/\sqrt{3} & 0 & 0 & 0 & -Qak_+ & p_2k_-/\sqrt{3} & 0 & -\sqrt{\frac{2}{3}}Qk_- & Qbk_+ \\
 & G_1-\lambda & \sqrt{\frac{2}{3}}Qa\hat{k}_z & 0 & -Q\hat{k}_z/\sqrt{3} & 0 & -\sqrt{\frac{2}{3}}Qb\hat{k}_z & 0 & 0 & -Qak_-/\sqrt{3} & -p_2k_+ & -\sqrt{\frac{2}{3}}Qk_- & 0 & Qbk_-/\sqrt{3} \\
 & & E_1-\lambda & p_4\hat{k}_z/\sqrt{3} & 0 & \sqrt{\frac{2}{3}}Qb\hat{k}_z & 0 & -Qak_+ & Qak_-/\sqrt{3} & 0 & \sqrt{\frac{2}{3}}p_4k_- & -Qbk_+ & Qbk_-/\sqrt{3} & 0 \\
 & & & -\lambda & -\sqrt{\frac{2}{3}}p_1\hat{k}_z & 0 & p_3\hat{k}_z/\sqrt{3} & p_2k_-/\sqrt{3} & p_2k_+ & \sqrt{\frac{2}{3}}p_4k_- & 0 & p_1k_-/\sqrt{3} & p_1k_+ & \sqrt{\frac{2}{3}}p_3k_- \\
 & & & & E_0-\lambda & 0 & 0 & 0 & \sqrt{\frac{2}{3}}Qk_- & -Qbk_+ & p_1k_-/\sqrt{3} & 0 & 0 & -Qak_+ \\
 & & & & & E_0-\lambda & \sqrt{\frac{2}{3}}Qa\hat{k}_z & \sqrt{\frac{2}{3}}Qk_- & 0 & -Qbk_-/\sqrt{3} & -p_1k_+ & 0 & 0 & -Qak_-/\sqrt{3} \\
 & & & & & & G_0-\lambda & Qbk_+ & -Qbk_-/\sqrt{3} & 0 & \sqrt{\frac{2}{3}}p_3k_- & -Qak_+ & Qak_-/\sqrt{3} & 0 \\
 & & & & & & & G_1-\lambda & 0 & 0 & \sqrt{\frac{2}{3}}p_2\hat{k}_z & 0 & Q\hat{k}_z/\sqrt{3} & 0 \\
 & & & & & & & & G_1-\lambda & \sqrt{\frac{2}{3}}Qa\hat{k}_z & 0 & -Q\hat{k}_z/\sqrt{3} & 0 & -\sqrt{\frac{2}{3}}b\hat{k}_z \\
 & & & & & & & & & E_1-\lambda & -p_4\hat{k}_z/\sqrt{3} & 0 & \sqrt{\frac{2}{3}}b\hat{k}_z & 0 \\
 & & & & & & & & & & -\lambda & \sqrt{\frac{2}{3}}p_1\hat{k}_z & 0 & -p_3\hat{k}_z/\sqrt{3} \\
 & & & & & & & & & & & E_0-\lambda & 0 & 0 \\
 & & & & & & & & & & & & E_0-\lambda & \sqrt{\frac{2}{3}}Qa\hat{k}_z \\
 & & & & & & & & & & & & & G_0-\lambda
\end{bmatrix}
\tag{2}
$$

We use the notation $a=\Delta'/(A+2B)$, $p_1=P_0+2\Delta' AP_1$, $p_2=P_1+\Delta' AP_0$, $p_3=P_0+2\Delta' BP_1$, $p_4=P_1-2\Delta' BP_0$. Here P_0, P_1, and Q are the interband matrix elements of momentum (defined in Ref. 1), and

$$\lambda=\varepsilon-\frac{\hbar^2k_\perp^2}{2m_0}-\frac{\hbar^2\hat{k}_z^2}{2m_0}-V(z), \tag{3}$$

where $\hat{k}_z=-i\partial/\partial z$ and $k_\perp^2=k_x^2+k_y^2$. The matrix (2) is written in the order $U_1,U_9,U_3,U_4,U_5,U_{13},U_7,U_8,U_2,U_{10},U_{11},U_{12},U_6,U_{14}$. It represents the eigenvalue problem for the energy ϵ and fourteen envelope functions $\Phi_l(z)$. Functions U_4 and U_{11} are associated with spin up and spin down components of the Γ_6 conduction band of our interest. We emphasize that the matrix element Q, which couples the Γ_8^v,Γ_7^v with the Γ_8^c,Γ_7^c multiplet, does not vanish because of the inversion asymmetry of the crystal. For this reason the five-level $\mathbf{k}\cdot\mathbf{p}$ model allows us to include the BIA mechanism of the spin splitting.

In order to reduce the fourteen coupled differential equations to the two equations for the Γ_6 conduction band, we observe that the matrix elements Q have only a secondary effect on the Γ_6^c band. Thus they can be included by iteration. We first neglect the Q terms in the matrix (2), as well as the free electron terms $\hbar^2\hat{k}_z^2/2m_0$ on the diagonal (which are small compared to the corresponding terms involving the effective electron mass). This allows us to express twelve of the fourteen envelope functions by the two functions Φ_4 and Φ_{11}. Then the complete equations (2) are used, from which the twelve functions are expressed by Φ_4 and Φ_{11}, now including also linear Q terms. The procedure is repeated to include quadratic terms k^2 and cubic terms k^3, as well as the terms proportional to $Q^2P_0^2k^4$. The resulting eigenvalue problem for the conduction band reads

$$\begin{pmatrix}\hat{A}+\hat{B}-\lambda & \hat{K}\\ \hat{K}^\dagger & \hat{A}-\hat{B}-\lambda\end{pmatrix}\begin{pmatrix}\Phi_1(z)\\ \Phi_2(z)\end{pmatrix}=0, \tag{4}$$

where

$$\hat{A}=-\frac{\hbar^2}{2}\frac{\partial}{\partial z}\frac{1}{m^*(z)}\frac{\partial}{\partial z}+\frac{\hbar^2k_\perp^2}{2m^*(z)}+V(z), \tag{5}$$

$$\hat{B}=i(k_x^2-k_y^2)\left(\frac{1}{2}\frac{\partial\gamma}{\partial z}+\gamma\frac{\partial}{\partial z}\right). \tag{6}$$

The effective mass is

$$\frac{m_0}{m^*(z)}=1+C-\frac{1}{3}\left[E_{P_0}\left(\frac{2}{\tilde{E}_0}+\frac{1}{\tilde{G}_0}\right)+E_{P_1}\left(\frac{2}{\tilde{G}_1}+\frac{1}{\tilde{E}_1}\right)+4\Delta'\sqrt{E_{P_0}E_{P_1}}\left(\frac{1}{\tilde{E}_1\tilde{G}_0}-\frac{1}{\tilde{E}_0\tilde{G}_1}\right)\right]. \tag{7}$$

Here

$$\tilde{E}_i=E_i-\varepsilon+V(z)+\frac{\hbar^2k_\perp^2}{2m_0}+\frac{\hbar^2\hat{k}_z^2}{2m_0} \tag{8}$$

and $\tilde{G}_i=\tilde{E}_i+\Delta_i$. Quantity C is the far band contribution to the effective mass, $E_{P_0}=2m_0P_0^2/\hbar^2$, and $E_{P_1}=2m_0P_1^2/\hbar^2$. The nondiagonal term in Eq. (4) consists of two parts

$$\hat{K}=\hat{K}_{\mathrm{SIA}}+\hat{K}_{\mathrm{BIA}}. \tag{9}$$

The first part, related to the structure inversion asymmetry, is

$$\hat{K}_{\mathrm{SIA}}=\frac{-ik_-}{\sqrt{2}}\frac{\partial\eta}{\partial z}, \tag{10}$$

where

$$\eta(z)=\frac{2}{3}\left[P_0^2\left(\frac{1}{\tilde{E}_0}-\frac{1}{\tilde{G}_0}\right)+P_1^2\left(\frac{1}{\tilde{G}_1}-\frac{1}{\tilde{E}_1}\right)-2\Delta' P_0P_1\left(\frac{1}{\tilde{E}_0\tilde{G}_1}+\frac{2}{\tilde{E}_1\tilde{G}_0}\right)\right]. \tag{11}$$

The second part, related to the bulk inversion asymmetry, is

$$\hat{K}_{\mathrm{BIA}}=-i\sqrt{2}k_xk_yk_-\gamma(z)-\sqrt{2}k_+\frac{\partial}{\partial z}\gamma(z)\frac{\partial}{\partial z}+\hat{K}_4, \tag{12}$$

where

$$\gamma(z)=\frac{4Q}{3}\left\{P_0P_1\left(\frac{1}{\tilde{G}_0\tilde{G}_1}-\frac{1}{\tilde{E}_0\tilde{E}_1}\right)-\Delta'\left[\frac{P_0^2}{\tilde{E}_0\tilde{G}_0}\left(\frac{2}{\tilde{E}_1}+\frac{1}{\tilde{G}_1}\right)-\frac{P_1^2}{\tilde{E}_1\tilde{G}_1}\left(\frac{2}{\tilde{G}_0}+\frac{1}{\tilde{E}_0}\right)\right]\right\} \tag{13}$$

and

$$\hat{K}_4=\sqrt{2}Q^2P_0^2[ik_-\hat{T}_1+ik_+(k_x^2-k_y^2)\hat{T}_2+k_xk_yk_+\hat{T}_3], \tag{14}$$

in which

$$\hat{T}_1=\frac{2}{9\tilde{G}_1}\left[\left(R\frac{\partial S}{\partial z}-3S\frac{\partial Z}{\partial z}\right)\frac{\partial^2}{\partial z^2}+\frac{k_\perp^2R}{2}\frac{\partial S}{\partial z}\right], \tag{15}$$

$$\hat{T}_2=\frac{1}{3\tilde{G}_0\tilde{G}_1}\frac{\partial S}{\partial z}, \tag{16}$$

$$\hat{T}_3=\frac{2}{3}\left(\frac{Z}{\tilde{G}_1}\frac{\partial}{\partial z}\frac{1}{\tilde{G}_0}-\frac{2}{\tilde{E}_0\tilde{E}_1}\frac{\partial}{\partial z}\frac{1}{\tilde{E}_0}\right). \tag{17}$$

Here $Z=1/\tilde{G}_0+1/\tilde{E}_0$, $R=2/\tilde{E}_0+1/\tilde{G}_0$, $S=1/\tilde{G}_0-1/\tilde{E}_0$. It can be seen that $\gamma(z)$ is proportional to the matrix element Q, which is nonzero because of the bulk inversion asymmetry of the crystal. The term $\hat{K}_4$ is of the fourth order in momentum and it contributes up to 12% to the spin splitting at high Fermi energies. It can be seen from the above formulas that the spin splitting of the Γ_6^c conduction band due to BIA is proportional to the spin-orbit energies of (Γ_8^v,Γ_7^v) and (Γ_8^c,Γ_7^c) bands and $\overline{\Delta}$.

The eigenvalue problem (4) describes the conduction band in the system illustrated in Fig. 1. The potential $V(z)$ is characterized by jumps (offsets) at the interfaces at $z=0$ and $z=a$. These offsets, when differenciated over z, result in the Dirac δ functions at $z=0$ and $z=a$. They have to be taken into account to satisfy the requirement that in a bound state the average electric field vanishes. The energy gaps E_i and the spin-orbit energies Δ_i have different values at both sides of the interfaces. On the other hand, it is assumed that the momentum matrix elements P_0, P_1, Q, and $\overline{\Delta}$ have the same values in different parts of the heterostructure. This is a reasonable approximation since the two materials composing the system are supposed to have the same symmetries of the band-edge periodic functions. In particular, it is well known that in various III-V compounds the value of P_0 is almost the same.

The inspection of the final results shows that the $\hat{B}$ terms in Eq. (4) give a negligible contribution to the spin splitting, so they are omitted in the following. In order to solve the set (1) one can apply general rules applying to 2×2 eigenvalue problems. First, the solutions for the diagonal terms are found. Since $\hat{B}$ is neglected, there is $\Phi_1(z)=\Phi_2(z)=\Phi(z)$. This envelope function obeys the usual boundary conditions

$$\Phi(z)\big|_{+_0}=\Phi(z)\big|_{-_0}, \tag{18}$$

$$\left(\frac{1}{m^*(z)}\frac{\partial\Phi}{\partial z}\right)\bigg|_{+_0}=\left(\frac{1}{m^*(z)}\frac{\partial\Phi}{\partial z}\right)\bigg|_{-_0}, \tag{19}$$

and similarly for the point $z=a$. Contrary to the statement in Ref. 12, we find that the spin-dependent boundary conditions do not influence much the calculated spin splitting related to the SIA mechanism. (That is, the boundary conditions do depend on the spin, but neglecting this dependence does not change much the final results.) For that reason we apply the simple boundary conditions (18) and (19). Having found the envelope function $\Phi(z)$ we calculate the average value of $\hat{k}_z$ and put it into the expressions for $\tilde{E}_i$ and $\tilde{G}_i$ [cf. Eq. (8)].

Calculating the average value of the nondiagonal terms $\hat{K}$ taken over $\Phi(z)$ we take into account the above mentioned Dirac δ functions at $z=0$ and $z=a$. After some manipulation, the average of $\hat{K}_{\rm SIA}$ is brought to the form

$$\langle\Phi|\hat{K}_{\rm SIA}|\Phi\rangle=\frac{-ik_-\sqrt{2}}{3}\left[\left\langle\Phi\left|\frac{-\partial V}{\partial z}D\right|\Phi\right\rangle+\Phi^2(0)C(0)-\Phi^2(a)C(a)\right], \tag{20}$$

where

$$D=\left\{P_0^2\left(\frac{1}{\tilde{E}_0^2}-\frac{1}{\tilde{G}_0^2}\right)+P_1^2\left(\frac{1}{\tilde{G}_1^2}-\frac{1}{\tilde{E}_1^2}\right)-2\Delta' P_0P_1\left[\frac{1}{\tilde{E}_0\tilde{G}_1}\left(\frac{1}{\tilde{E}_0}+\frac{1}{\tilde{G}_1}\right)+\frac{2}{\tilde{E}_1\tilde{G}_0}\left(\frac{1}{\tilde{E}_1}+\frac{1}{\tilde{G}_0}\right)\right]\right\}. \tag{21}$$

When integrating the first term over the regions I, II, and I (see Fig. 1), one has to take in D the corresponding values of the gaps E_i and the spin-orbit energies Δ_i. The points $z=0$ and $z=a$ are excluded from the integration. The quantities $\Phi(0)$ and $\Phi(a)$ are the values of the envelope function at $z=0$ and $z=a$, respectively, and

$$C(0)=[\mathrm{II}]_0-[\mathrm{I}]_0, \tag{22}$$

$$C(a)=[\mathrm{II}]_a-[\mathrm{I}]_a, \tag{23}$$

in which, for example,

$$[\mathrm{II}]_0=\left[\frac{P_0^2\Delta_0^{\rm II}}{\tilde{E}_0^{\rm II}\tilde{G}_0^{\rm II}}-\frac{P_1^2\Delta_1^{\rm II}}{\tilde{E}_1^{\rm II}\mathrm{G}_1^{\rm II}}-2\Delta' P_0P_1\left(\frac{1}{\tilde{E}_0^{\rm II}\tilde{G}_1^{\rm II}}+\frac{2}{\tilde{E}_1^{\rm II}\tilde{G}_0^{\rm II}}\right)\right]_0. \tag{24}$$

The symbol $[\mathrm{II}]_0$ means that the values $\tilde{E}_i$ and $\tilde{G}_i$ should be taken for the region II, while the subscript 0 or a indicates that the value of the potential $V(z)$ in $\tilde{E}_i$ and $\tilde{G}_i$ should be taken at the point 0 or a from the left or from the right, depending on the region. Thus $V^{\rm II}(0)=0, V^{\rm I}(0)=V_B, V^{\rm II}(a)=V(a), V^{\rm I}(a)=V(a)+V_B$. It can be seen from the above formulas that the spin splitting in the Γ_6 conduction band due to the SIA mechanism is proportional to the spin-orbit energies in the (Γ_8^v,Γ_7^v) and (Γ_8^c,Γ_7^c) bands.

To make connection with the claims that the SIA spin splitting is proportional to the average electric field, we transform the above expression observing that the electric field in the conduction band is $Eq=-\partial V/\partial z+V_B\delta(z)-V_B\delta(z-a)$, where the first term excludes the points $z=0$ and $z=a$. Since the envelope function $\Phi(z)$ is nonzero mostly in the well (region II), we add and subtract $V_B\Phi^2(0)D(0)$ and $V_B\Phi^2(a)D(a)$ from the right-hand side of Eq. (20), and obtain

$$\langle\Phi|\hat{K}_{\rm SIA}|\Phi\rangle=\frac{-ik_-\sqrt{2}}{3}\left[\left\langle\Phi\left|\frac{-\partial V}{\partial z}D_i\right|\Phi\right\rangle+V_B\Phi^2(0)D(0)-V_B\Phi^2(a)D(a)\right]+\frac{-ik_-\sqrt{2}}{3}\{\Phi^2(0)[C(0)-V_BD(0)]-\Phi^2(a)[C(a)-V_BD(a)]\}, \tag{25}$$

where

$$D(0)=\left\{P_0^2\left[\frac{1}{(\tilde{E}_0^{\rm II})^2}-\frac{1}{(\tilde{G}_0^{\rm II})^2}\right]+P_1^2\left[\frac{1}{(\tilde{G}_1^{\rm II})^2}-\frac{1}{(\tilde{E}_1^{\rm II})^2}\right]-2\Delta' P_0P_1\left[\frac{1}{\tilde{E}_0^{\rm II}\tilde{G}_1^{\rm II}}\left(\frac{1}{\tilde{E}_0^{\rm II}}+\frac{1}{\tilde{G}_1^{\rm II}}\right)+\frac{2}{\tilde{E}_1^{\rm II}\tilde{G}_0^{\rm II}}\left(\frac{1}{\tilde{E}_1^{\rm II}}+\frac{1}{\tilde{G}_0^{\rm II}}\right)\right]\right\}_0. \tag{26}$$

The subscript 0 in Eq. (26) means that one should put $V^{\rm II}(0)=0$. The quantity $D(a)$ has the identical form to that

given by Eq. (26) [i.e., it contains the energies from the II region, but the potential value is $V^{II}(a)=V(a)$]. Since to a good approximation there is $D_i \approx D_0 \approx D_a$, the expression in the first square bracket of Eq. (25) is approximately proportional to the average electric field E. However, we deal with a bound state, so that this average field is near zero and, as we show below, this term contributes only few percent to the total SIA spin splitting. Thus, we are left with the dominant second term in Eq. (25), which requires only the knowledge of the band parameters on both sides of the interfaces and of the envelope function at the interfaces.

The total spin splitting, due to both bulk and structure asymmetries, is

$$\Delta\varepsilon = 2(\langle\Phi|\hat{K}|\Phi\rangle\langle\Phi|\hat{K}^{\dagger}|\Phi\rangle)^{1/2}. \tag{27}$$

One can now consider the spin splitting for main directions of $\mathbf{k}_F$. We have

$$\hat{K}^{\pm}(1\bar{1}0) = \frac{(1\pm i)}{\sqrt{2}} k_{\perp}\left[\pm\frac{1}{2}\frac{\partial\eta(z)}{\partial z} + \frac{k_{\perp}^2\gamma(z)}{2} + \frac{\partial}{\partial z}\gamma(z)\frac{\partial}{\partial z} \mp Q^2 P_0^2\left(\hat{T}_1 + \frac{k_{\perp}^2}{2}\hat{T}_3\right)\right], \tag{28}$$

where the upper signs are for $\mathbf{k}\|[110]$ and lower for $\mathbf{k}\|[1\bar{1}0]$. It can be seen that if Q^2 term is neglected (it gives a contribution of few percent), there is $\Delta\varepsilon_{\mathrm{BIA}}(110) = \Delta\varepsilon_{\mathrm{BIA}}(1\bar{1}0)$. For $\mathbf{k}\|[100]$

$$\hat{K}(100) = -ik_{\perp}\left[\frac{1}{2}\frac{\partial\eta(z)}{\partial z} - i\frac{\partial}{\partial z}\gamma(z)\frac{\partial}{\partial z} - Q^2P_0^2(\hat{T}_1 + k_{\perp}^2\hat{T}_2)\right]. \tag{29}$$

Finally, we calculate the splitting averaging over $\mathbf{k}$ directions in the interface plane (k_x, k_y). This gives (neglecting Q^4 terms)

$$\Delta\varepsilon(k_{\perp}) = 2k_{\perp}\left[\frac{1}{4}\left\langle\Phi\left|\frac{\partial\eta(z)}{\partial z}\right|\Phi\right\rangle^2 + \frac{k_{\perp}^4}{8}\langle\Phi|\gamma(z)|\Phi\rangle^2 + \left\langle\Phi\left|\frac{\partial}{\partial z}\gamma(z)\frac{\partial}{\partial z}\right|\Phi\right\rangle^2 + \frac{k_{\perp}^2}{2}\langle\Phi|\gamma(z)|\Phi\rangle \times\left\langle\Phi\left|\frac{\partial}{\partial z}\gamma(z)\frac{\partial}{\partial z}\right|\Phi\right\rangle - \frac{Q^2P_0^2}{2}\left\langle\Phi\left|\frac{\partial\eta(z)}{\partial z}\right|\Phi\right\rangle \times\left\langle\Phi\left|\hat{T}_1 + \frac{k_{\perp}^2}{2}\hat{T}_3\right|\Phi\right\rangle\right]^{1/2}. \tag{30}$$

If small Q^2 term is neglected in Eq. (30), the expression under the square root decouples into separate contributions from SIA and BIA mechanisms.

III. RESULTS AND DISCUSSION

We apply the above formalism to the GaAs/$Ga_{0.67}Al_{0.33}$Asheterojunction by specifying the potential and the band parameters on both sides of the interfaces. We take the following band parameters for GaAs (see Ref. 1): $E_0=-1.519$ eV, $G_0=-1.86$ eV, $E_1=2.969$ eV, $G_1=3.14$ eV, $\bar{\Delta}=-0.061$ eV, $E_{P_0}=27.86$ eV, $E_{P_1}=2.36$ eV, $E_Q=15.56$ eV, $C=-2.31$. For $Ga_{0.67}Al_{0.33}$. As we take $E_0=-1.992$ eV, $G_0=-2.297$ eV, $E_1=2.641$ eV, $G_1=2.812$ eV, $C=-1.77$. As mentioned above, the values of the matrix elements P_0, P_1, Q, and $\bar{\Delta}$ are taken to be the same as for GaAs. The width of the well is $a=180$ Å and the offset value for the above chemical composition is $V_b=0.264$ eV.

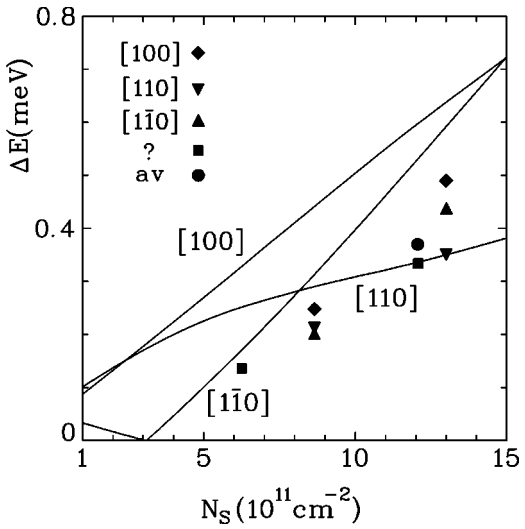

FIG. 4. The same as in Fig. 3, but with the theoretical curves calculated for $N_{\mathrm{depl}}=1\times10^{11}\,\mathrm{cm}^{-2}$.

The potential $V(z)$ and the envelope function $\Phi(z)$ are found in a self-consistent way neglecting the off-diagonal terms in Eq. (4) and taking into account the exchange-correlation effects.[27] This is done for given values of the 2D electron density N_s and the depletion density N_d. Above $N_s=1.2\times10^{11}\,\mathrm{cm}^{-2}$ the electrons begin to occupy the excited electric subband, which has to be accounted for in the calculation of $\mathbf{k}_F$ for the ground subband of our interest. The spin splittings are then calculated according to the formulas given above.

In Fig. 2 we show the calculated spin splitting of the conduction subband averaged over the $\mathbf{k}_{\perp}$ directions [i.e., as described by Eq. (30)]. The solid curves show the theoretical splittings related to BIA and SIA mechanisms, and the total theoretical splitting due to both mechanisms. It can be seen that in GaAs/$Ga_{0.67}Al_{0.33}$As system BIA predominates at lower N_s values (below $6\times10^{11}\,\mathrm{cm}^{-2}$), while at higher N_s the SIA mechanism takes over. The resulting total splitting increases almost linearly with N_s. Full points indicate the experimental Raman data of Refs. 17 and 18. (As mentioned in the Introduction, these values are twice lower than those quoted in Refs. 12 and 13). A comparison of the experiment with the theory for the average splitting is only tentative since the data are obtained for specific directions of $\mathbf{k}$ (see below).

We are now in a position to evaluate relative importance of the two terms contributing to the SIA spin splitting [see Eq. (25)]. The first term, approximately proportional to the average electric field in the conduction band, contributes

only about 3% to the total SIA splitting $\Delta\varepsilon_{\mathrm{SIA}}$. This explicitly disproves the claim that the SIA splitting is proportional to the average electric field. (Similar results are obtained for $In_{0.53}Ga_{0.47}As/In_{0.52}Al_{0.48}As$ heterostructure, see Ref. 25). It should be emphasized again that the average electric field in the bound state is not exactly zero only due to the effective mass differences in various parts of the structure.

A few remarks concerning comparison with our previous results are in order. The present theoretical values of the spin splitting for the SIA mechanism are somewhat lower than those of Ref. 12. This difference is due to several reasons. First, the present more exact theory (based on the reduction of the 14×14 problem to the 2×2 problem by substitution) gives lower values than the previous theory based on the perturbation approach. Second, the calculation shown in Fig. 2 assumes $N_d=0$,while that assumed in Ref. 12 was $N_d=8\times10^{10}\,\mathrm{cm}^{-2}$. (For the influence of N_d on the splitting, see below.) Third, the present calculation considers two interfaces, whereas that of Ref. 12 considered a single heterojunction, which resulted in a stronger inversion asymmetry. In addition, due to an error in programming, the SIA and BIA mechanisms were not combined correctly in Ref. 12. The correct combination is shown in Fig. 2.

Figure 3 shows the calculated spin splitting (combined BIA and SIA mechanisms) for three directions of $\mathbf{k}$, taking the value of $N_d=0$. In Raman experiments one can choose $\mathbf{k}$ direction, at least approximately, by applying a proper light polarization.[17,18] The corresponding experimental data are marked in Fig. 3 by various full points. It can be seen that the theory correctly describes the main anisotropy between [110] and $[1\bar{1}0]$ directions and, in particular, the crossover between the corresponding splittings for increasing N_s. The experimental anisotropy is weaker than the theoretical one, which can be attributed to the fact that in Raman experiments the appropriate light polarization fixes $\mathbf{k}$ direction not exactly but only preferentially.[28] The fact that the splittings for [110] and $[1\bar{1}0]$ directions is not the same, is by itself a proof that both SIA and BIA mechanisms contribute to the effect, since BIA alone gives almost the same values for these two $\mathbf{k}$ directions [see Eq. (28)]. As to the comparison of the present theory with our previous calculations, all the above remarks concerning the average splitting apply also here. It can be added that fitting the previous theory to the incorrect experimental readings (twice as high) forced us to assume in Ref. 13 a very high value of $N_d=3.5\times10^{11}\,\mathrm{cm}^{-2}$, whereas the data shown in Fig. 3 are well described by $N_d=0$. The splitting for $[1\bar{1}0]$ direction of $\mathbf{k}$ changes sign around $N_s\approx3.5\times10^{11}\,\mathrm{cm}^{-2}$. (This effect was already visible in Fig. 2 of Ref. 13, but it occurred around $N_s\approx1.5\times10^{11}\,\mathrm{cm}^{-2}$ since it depends on the value of N_d, which was assumed to be quite high.)

The value of the depletion density N_d influences the penetration of the subband wave function into GaAlAs region (see Fig. 1) which, in turn, affects the splitting. To illustrate the sensitivity of the theory to the value of N_d, we show in Fig. 4 the theoretical curves calculated for $N_d=1\times10^{11}\,\mathrm{cm}^{-2}$ and compared to the same data. It can be seen that the increase of N_d affects differently the splittings for various directions, that for $\mathbf{k}_F\|[110]$ being affected more than the other two. The difference between the present procedure and the perturbation theory of the third order (we do not present explicitly the latter calculations) grows with increasing N_s. For $N_s=1.5\times10^{12}\,\mathrm{cm}^{-2}$ the perturbation theory gives the spin splittings around 15% higher than those shown in Fig. 3 for [100] and $[1\bar{1}0]$ directions and 20% higher for [110] direction. The growing difference between the ''substitutional'' and the perturbative (third order) theory with increasing N_s can be qualitatively understood by observing that the spin splitting due to inversion asymmetry is a nonparabolic effect in the band structure, which becomes bigger with increasing energy distance from the conduction band edge (i.e., with increasing Fermi energy). At larger values of E_F, higher powers than the third become of importance, which is taken into account by the present approach.

Finally, it is of interest to compare the results of the five-level $\mathbf{k}\cdot\mathbf{p}$ model applied here to those of the simpler three-level model (see Ref. 25). It has been convincingly argued before that, since GaAs is not a narrow-gap material, 5LM is distinctly better than 3LM for higher Fermi energies. Also, as already mentioned above, 5LM includes naturally the effects of bulk inversion asymmetry due to the appearance of the matrix element Q. On the other hand, using the 3LM approach, one has to put ''by hand'' the terms related to BIA into the initial matrix (see Ref. 25). As to the comparison of the splitting values calculated by the two models, they depend on the direction on $\mathbf{k}_F$. In general the 3LM theory gives a somewhat smaller anisotropy than the results of 5LM treatment shown in Fig. 3. For $\mathbf{k}_F\|[110]$ the spin splitting according to 3LM at $N_s=1.5\times10^{12}\,\mathrm{cm}^{-2}$ is about 20% higher than that given in Fig. 3. For other directions of $\mathbf{k}_F$ the differences between the results of the two models are smaller.

Concerning the influence of an external electric field on the spin splitting of conduction subbands in III-V heterostructures,[21–23] it should be emphasized that the external field affects the splitting neither by changing the average value of the field in the well (the latter must remain near zero in a bound state), nor by controlling the spin-orbit interaction, but by changing the Fermi wave vector and the asymmetry of the quantum well. The main difficulty in describing such data is an unknown distribution of the field in the structure.

IV. SUMMARY

A theory of the spin splitting of conduction subbands in $GaAs\text{-}Ga_{1-x}Al_xAs$ heterostructures due to bulk and structure inversion asymmetries is developed, using the five-level $\mathbf{k}\cdot\mathbf{p}$ model of the band structure for GaAs-type materials. The five-level model allows one to treat naturally the BIA mechanism of the spin splitting. This model is solved by substitution with the use of iteration, providing a more precise description than the previous perturbative methods. It is shown explicitly that the spin splitting due to SIA is not proportional to the average electric field in the conduction band, since the latter is almost zero in a bound state. The theory is used to describe available Raman data on the spin splitting in $GaAs\text{-}Ga_{0.67}Al_{0.33}As$ heterostructures, correcting the previously quoted experimental values. The theory describes the experimental splittings quite well (both their absolute values and their anisotropy for different directions of the Fermi

wave vector) without adjustable parameters. It is concluded that the spin splitting in the above system is dominated by the BIA mechanism at lower electron densities and by the SIA mechanism at higher densities. The results of the complete theory are used to discuss simpler treatments: the perturbative approach to the five-level $\mathbf{k}\cdot\mathbf{p}$ model and the three-level $\mathbf{k}\cdot\mathbf{p}$ model.

Note added in proof. A recent paper by Wissinger *et al.*[29] treats the same subject. The procedure of this paper is based on the multiband envelope function approach of Winkler and Roessler.[10] No details of the calculation are given, but the band parameters used in Ref. 29 as well as the final results for the spin splitting of the ground electric subband in GaAs/$Ga_{0.7}Al_{0.3}As$ heterostructures are similar to ours.

ACKNOWLEDGMENTS

I am grateful to Dr. D. Jusserand and Dr. D. Richards for turning my attention to the fact that the experimental spin splittings quoted in Refs. 12 and 13 are twice too large, and to Professor G. Abstreiter for the discussion concerning experimental aspects of the Raman measurements. This work was supported in part by the Polish Committee for Scientific Research under Grant No. 2P03B13911.

[1] P. Pfeffer and W. Zawadzki, Phys. Rev. B **41**, 1561 (1990).
[2] Y. A. Bychkov and E. I. Rashba, J. Phys. C **17**, 6039 (1984).
[3] F. J. Ohkawa and Y. Uemura, J. Phys. Soc. Jpn. **37**, 1325 (1974).
[4] A. Darr, J. P. Kotthaus, and T. Ando, in *Proceedings of the 13th International Conference on the Physics of Semiconductors*, Rome, 1976, edited by F. G. Fumi (North-Holland, Amsterdam, 1976), p. 774.
[5] R. Lassnig, Phys. Rev. B **31**, 8076 (1985).
[6] F. Malcher, G. Lommer, and U. Roessler, Superlattices Microstruct. **2**, 267 (1986).
[7] P. Sobkowicz, Semicond. Sci. Technol. **5**, 183 (1990).
[8] G. Bastard, J. A. Brum, and R. Ferreira, *Solid State Physics*, edited by H. Ehrenreich and D. Turnbull (Academic, New York, 1991), Vol. 44, p. 229.
[9] R. Eppenga and M. F. H. Schurmann, Phys. Rev. B **37**, 10 923 (1988).
[10] R. Winkler and U. Roessler, Phys. Rev. B **48**, 8918 (1992).
[11] E. A. de Andrada e Silva, G. C. La Rocca, and F. Bassani, Phys. Rev. B **50**, 8523 (1994) [a modified version by the same authors is: Phys. Rev. B **55**, 16 293 (1997)].
[12] P. Pfeffer and W. Zawadzki, Phys. Rev. B **52**, R14 332 (1995).
[13] P. Pfeffer, Phys. Rev. B **55**, R7359 (1997).
[14] D. Stein, K. v. Klitzing, and G. Weimann, Phys. Rev. Lett. **51**, 130 (1983).
[15] P. D. Dresselhaus, C. M. A. Papavassiliou, R. G. Wheeler, and R. N. Sacks, Phys. Rev. Lett. **68**, 106 (1992).
[16] W. Knap *et al.*, Phys. Rev. B **53**, 3912 (1996).
[17] B. Jusserand, D. Richards, G. Allan, C. Priester, and B. Etienne, Phys. Rev. B **51**, 4707 (1995).
[18] D. Richards, B. Jusserand, G. Allan, C. Priester, and B. Etienne, Solid-State Electron. **40**, 127 (1996).
[19] B. Das *et al.*, Phys. Rev. B **39**, 1411 (1989).
[20] J. Luo, H. Munekata, F. F. Fang, and P. J. Stiles, Phys. Rev. B **41**, 7685 (1990).
[21] J. P. Heida *et al.*, Phys. Rev. B **57**, 11 911 (1998).
[22] J. Nitta, T. Akazaki, H. Takayanagi, and T. Enoki, Phys. Rev. Lett. **78**, 1335 (1997).
[23] G. Engles, J. Lange, Th. Schapers, and H. Luth, Phys. Rev. B **55**, R1958 (1997).
[24] T. Ando, A. B. Fowler, and F. Stern, Rev. Mod. Phys. **54**, 437 (1982).
[25] P. Pfeffer and W. Zawadzki, Phys. Rev. B **59**, R5312 (1999).
[26] F. H. Pollak, C. W. Higginbotham, and M. Cardona, J. Phys. Soc. Jpn. Suppl. **21**, 20 (1966).
[27] L. Hedin and B. I. Lundqvist, J. Phys. C **4**, 2064 (1971).
[28] G. Abstreiter (private communication).
[29] L. Wissinger *et al.*, Phys. Rev. B **58**, 15 375 (1998).